

HOLES IN THE MOON: COPERNICUS CRATER COLLAPSE PITS. A. N. M. Lang¹ and T.K.P Gregg¹.¹Department of Geology, 126 Cooke Hall, University at Buffalo, Buffalo, NY (anlang@buffalo.edu).

Introduction: As lunar exploration advances, it will be important to find safe places for astronauts to shelter. Collapse pits could protect astronauts from dangerous surface conditions [1] while providing access to scientific targets at depth. Copernicus crater hosts 35 previously discovered pits [2], the majority of which are present in previously mapped impact melt [3]. Many of these pits are aligned with, or contained within, linear to arcuate depressions (Fig. 1). Careful inspection of the Lunar Reconnaissance Orbiter's Narrow Angle Camera (NAC) [4] has revealed previously unmapped pits. By mapping and analyzing all collapse pits, we can better infer their subsurface connectedness and suitability for habitation.

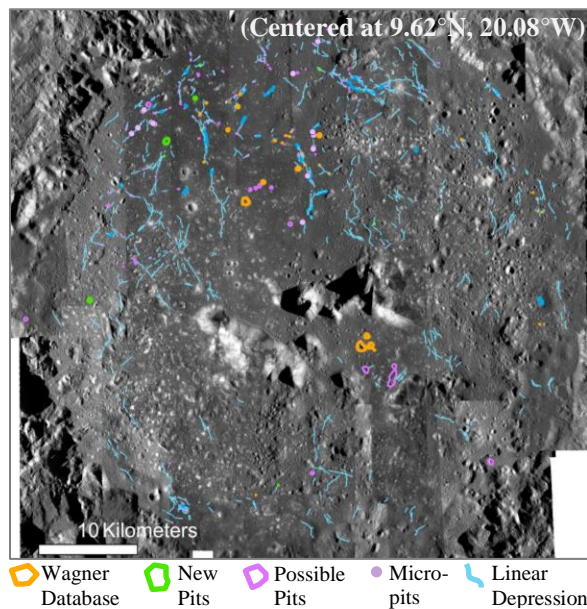


Figure 1. Map of collapse pits (colored polygons) and linear depressions (blue lines) on Copernicus crater's floor, mapped on mosaiced NAC images (1 – 0.5m/px).

Methods: Mosaiced NAC images were used as the base map because the typical pit size is tens to hundreds of meters across. After importing all NACs into ArcGIS, the previously discovered pits were mapped with the help of the PitScan database [3] (R. Wagner, personal commun., 2019).

We developed a scoring system (Table 1) to quantify the probability that a feature is a collapse pit, enabling us to identify and map additional pits that were not included on the PitScan database. Our scoring system was verified against the PitScan pits; all PitScan pits have a score ≥ 5 .

Table 1. Morphologic characteristics of lunar collapse pits. A score of ≥ 5 indicates a collapse pit.

Excellent (5)	Very Good (4)	Good (2)	Fair (1)
Wall not visible all the way to floor	$\geq 75\%$ exposure of roof material*	Deviation from circularity	Proximity to other pits
		Abrupt transition from wall to floor	Concentration of boulders around rim
		No raised rim	No ejecta

*Roof material is identified by outcrops of cliff-forming material at the pit rim.

Basic statistical analysis was conducted using the PitScan database. The database contains the average depth (from three separate shadow calculations) and the maximum and minimum pit diameter. An additional variable, circularity, was created by dividing the minimum diameter by the maximum diameter).

While mapping PitScan pits, we identified and mapped previously unknown pits. We also mapped linear depressions.

Preliminary results: Mapping and scoring newly discovered features continues, but some preliminary interpretations can be made based on the current map and statistical analysis; see Figure 2 for preliminary statistical results.

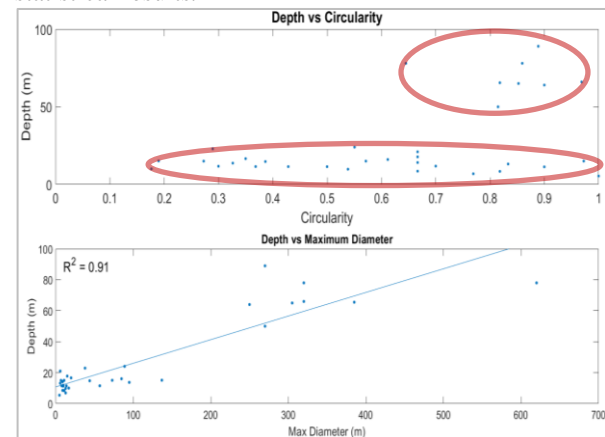


Figure 2. Top graph shows two distinct morphologic groups (highlighted in red); note that deeper pits tend to be more circular. Bottom graph shows the relationship between depth and max diameter, along with the best-fit line ($R^2 = 0.91$).

Pit Distribution. Most pits, including newly discovered pits, are located within previously mapped impact melt [3]. Pits also tend to be near other pits or linear depressions, rather than spatially isolated. Pits

that do not lie within linear depressions tend to be one to two diameters from another pit or depression.

Pit Morphology. There are several classes of pit morphology (Fig. 3). Large pits (100s of meters in diameter) tend to have steep, irregular walls and interiors blanketed with boulders. Medium pits (10s of meters in diameter) generally display a clear break in slope between the roof and walls (when not hidden by overhangs), and in some pits a debris-covered floor can be seen through the opening. Others have a trapdoor morphology similar to the pit in Lacus Mortis [5]. Small pits (<10 m diameter) are too small to properly score, but they are almost always within linear depressions and tend to have higher albedo slopes without a raised rim when compared with similarly sized impact craters. The lack of raised rim and steep walls aligns with descriptions of larger pits.

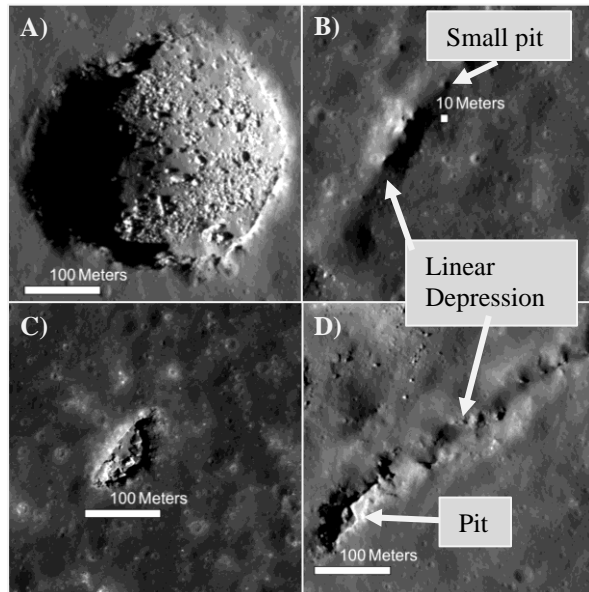


Figure 3. A) A large pit with an internal boulder field (10.20°N, 20.00°W). B) A small pit within a linear depression (10.24°N, 20.61°W). C) A medium pit with internal debris and an overhang (10.32°N, 20.38°W). D) A medium pit with internal debris within a linear depression (10.36°N, 20.25°W). All images were captured at 1:3,000 view in ArcGIS.

Pits Near Central Peak. Three pits near Copernicus crater's central peak complex have a unique morphology (Fig. 4). They are the largest pits in Copernicus crater, and Clementine data reveal a higher titanium content (or bright slopes) [6] than other pits on the crater floor. Nearby, there is a smaller trapdoor pit. Due to their uniqueness, these pits require more study.

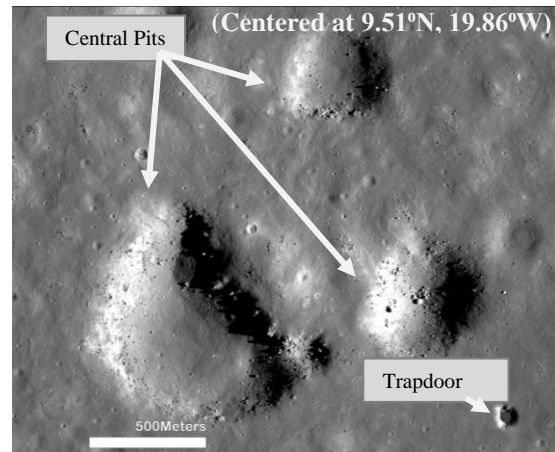


Figure 4. Three large pits near the central peak complex with rubbly edges. The bottom-left pit is the largest pit in Copernicus. Note the trapdoor pit in the bottom right, within one diameter distance from the nearest pit.

Linear Depression Orientation. Where linear depressions and large (≥ 1 km basal diameter) hills occur, the depressions tend to radiate out from the hill. These are concentrated in impact melt [3] but are also found in hummocky areas of the crater floor. Within impact melt, linear depressions tend to cross each other at 90° - 90° and 60° - 120° angles [7].

Preliminary Interpretations: Because pits tend to be associated with linear depressions, and small pits are always associated with them, it is likely shallow linear depressions collapse further and evolve into pits and pit chains with time.

Ongoing work: After mapping and scoring the rest of Copernicus crater's floor, spatial analysis will be conducted using ArcGIS to confirm visual distribution patterns.

Acknowledgments: The authors are grateful to Robert Wagner for providing the work in progress PitScan database. PILOT was used to process all NAC (courtesy of NASA/GSFC/ASU) images, which makes use of the Planetary Data System (PDS).

References: [1] Deran, A. et al. (2016) *LPSC XXXVII*, Abstract #1903. [2] Wagner, R. V. and Robinson, M. S. (2014) *Icarus* 237, 52-60. [3] Howard, K. (1975) USGS I-Map Ser. 840, 1:250,000. [4] Robinson, M.S et al. (2010) *Space Sci. Rev.* 150(1-4), 81-124. [5] Hong, I. S., et al. (2015) *J. Astron. Space Sci.* 32(2), 113-120. [6] Lucey, P. G. et al. (2000) *J. Geophys. Res.-Planet.* 105(8), 20297-20305. [7] Waldron, J. and Morgan, S. (2020) *Geological Structures: a Practical Introduction*, 123-129.